Bioorganic & Medicinal Chemistry Letters 22 (2012) 472–475

Contents lists available at SciVerse ScienceDirect

Bioorganic & Medicinal Chemistry Letters

journal homepage: www.elsevier.com/locate/bmcl

Fused thiophene derivatives as MEK inhibitors

Victoria E. Laing [a,*], Daniel C. Brookings [a], Rachel J. Carbery [a], Jose Gascon Simorte [a], Martin C. Hutchings [a], Barry J. Langham [a], Martin A. Lowe [a], Rodger A. Allen [b], Joanne R. Fetterman [c], James Turner [a], Christoph Meier [b], Jeff Kennedy [b], Mark Merriman [b]

[a] Department of Medicinal Chemistry, UCB Pharma, 216 Bath Road, Slough, Berkshire SL1 3WE, UK
[b] Department of Biology, UCB Pharma, 216 Bath Road, Slough, Berkshire SL1 3WE, UK
[c] Department of Pharmacology, UCB Pharma, 216 Bath Road, Slough, Berkshire SL1 3WE, UK

ARTICLE INFO

Article history:
Received 7 September 2011
Revised 26 October 2011
Accepted 28 October 2011
Available online 6 November 2011

Keywords:
MEK
Non-ATP competitive MEK inhibitor
Allosteric MEK inhibitor

ABSTRACT

A number of novel fused thiophene derivatives have been prepared and identified as potent inhibitors of MEK. The SAR data of selected examples and the in vivo profiling of compound **13h** demonstrates the functional activity of this class of compounds in HT-29 PK/PD models.

The Ras/Raf/MEK/ERK mitogen-activated protein (MAP) kinase signaling pathway is responsible for the coordination and regulation of cell growth and differentiation in response to extracellular stimulation.[1,2] Raf-activated MAPK/ERK kinase (MEK 1,2 a dual specificity tyrosine/threonine protein kinase) activates the MAP kinase known as extracellular signal-regulated kinase (ERK) through phosphorylation of key tyrosine and threonine residues.[3] The Raf/MEK/ERK cascade plays a central role in the regulation of cell proliferation and survival and this pathway is deregulated in a high number of human cancers. Inhibition of this signalling cascade is, therefore, an attractive target for small molecule drug development.[4] In particular non-ATP competitive MEK inhibitors have been reported to exhibit exquisite selectivity, and there are several compounds advancing into clinical development.[5] We report in this letter our efforts to identify novel, ATP non-competitive, inhibitors of MEK as potential oncology therapeutics.

Pfizer have reported the clinical development of the non-ATP competitive MEK inhibitor **PD0325901**, Figure 1.[6] Phase I studies demonstrated significant target engagement with a decrease in ERK phosphorylation observed in >60% of tumour biopsies collected post treatment. However extended phase I evaluation showed unacceptable ocular toxicity and a pilot phase II clinical trial in previously treated patients with non-small cell lung cancer demonstrated limited efficacy and the trial was consequently discontinued. During the discovery of **PD0325901** Pfizer disclosed the X-ray co-crystal structure of MEK with the closely related analogue **PD318088**.[7]

The structure provides valuable insight into the mechanism of non-ATP competitive inhibition of MEK, in particular **PD318088** binds in a novel binding pocket separate from, but adjacent to the Mg-ATP site with the key feature being an electrostatic interaction between the aryl iodide of **PD318088** and the carbonyl of Val127.

Our attempts to identify novel MEK inhibitors began from a desire to utilise proprietary chemical scaffolds developed for other kinase targets.[8,9] We initially hypothesised that a thiazole such as **1** Figure 2, could act as a non-ATP competitive MEK inhibitor.

We reasoned that the aryl iodide would form the key electrostatic interaction with Val127 whilst the carbonyl function would form a hydrogen bond with the backbone NH of Ser212 analogous to the 4-fluoro in **PD318088**.[11,12] Consequently we were delighted to discover that upon synthesis of **1** and testing in an in vitro Raf/MEK/ERK cascade assay[10] compound **1** displayed promising inhibitory activity (IC_{50} 946 nM). To improve both the potency and physiochemical properties of **1** we targeted the 3-carboxythiophene

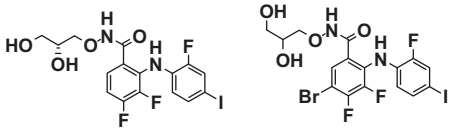

Figure 1. Structures of **PD0325901** which entered clinical development and **PD0318088** which was reported in co-crystallization with MEK1, Mg^{2+} and ATP.

* Corresponding author.
E-mail address: victoria.jackson@ucb.com (V.E. Laing).

0960-894X/$ - see front matter © 2011 Elsevier Ltd. All rights reserved.
doi:10.1016/j.bmcl.2011.10.105

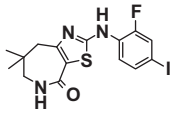

1

Figure 2. Compound **1**, 2-(2-Fluoro-4-iodo-phenylamino)-7,7-dimethyl-5,6,7,8-tetrahydro-thiazolo[5,4-*c*]azepin-4-one.

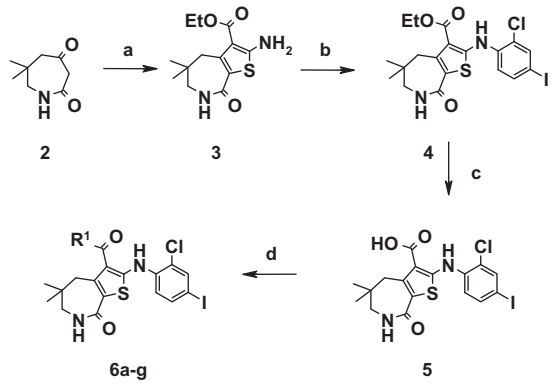

Scheme 1. Reagents and conditions: (a)S_8, EtOH, morpholine, ethylcyanoacetate, 45 °C, 51%; (b) Cs_2CO_3, DMF, 2-Chloro-1-fluoro-4-iodobenzene, 65 °C, 25%; (c) LiOH, THF, H_2O, reflux, 79%; (d) amine R^1, EDC, NMM, HOBt, DMF, rt, 40–60%.

analogues **6** (Scheme 1). We hypothesised that substitution at the thiophene 3 position would allow access to the ATP binding region offering potential for increased potency and the introduction of polar functionality to improve the physiochemical properties of the molecules. Therefore, initial efforts were made to synthesize a series of thiophene-3-carboxamides as described in Scheme 1 with selected SAR data in Table 1.

Gewald[13–15] reaction of 6,6-dimethyl-azepane-2,4-dione, **2** gave thiophene intermediate **3** in an acceptable yield (51%). Introduction of the aniline substituent relied on a poor yielding nucleophilic displacement of 2-chloro-1-fluoro-4-iodobenzene with **3** (25% yield). Hydrolysis of the ester **4** provided the acid **5** in 79% yield. The resultant acid could then be simply reacted with a variety of substituted amines to provide the carboxamides **6a–6g** in yields ranging from 40–60%.

For SAR determination, all compounds were evaluated in a coupled Raf-MEK-ERK IMAP cascade assay.[10] Constituently active Raf phosphorylates and activates MEK which in turn phosphorylates ERK which phosphorylates a fluorescent labelled Erk-tide substrate, measurement of which provides the basis of the assay. In this way the activity of the compounds against either active and/or inactive MEK can be deduced. Compounds showing potency in the primary assay were further evaluated by measuring both the inhibition of ERK phosphorylation and the proliferation of HT-29 colon cancer cell lines.

Incorporation of the 3-thiophene ester **4** did not improve potency compared to thiazole **1**. However the simple primary amide, **6a** demonstrated much improved activity in the cascade assay (13 nM) which translated into potent inhibition of pERK in HT-29 cells (92 nM). However, poor aqueous solubility precluded further profiling of **6a**. Secondary and tertiary amides **6b** and **6c** improved solubility but did not increase inhibition in the cascade assay. Polar polyhydroxylated amide side chains were synthesized and **6d** showed good initial activity in the cascade assay and against pERK (28 and 43 nM), but this activity was not maintained in the HT-29 proliferation assay. Hydroxamate esters had previously been reported by Pfizer[16] to be beneficial in improving cell potency and solubility and therefore we endeavoured to synthesize hydroxamic esters in our thiophene series. Pleasingly the dihydroxypropyl hydroxamate **6f** revealed a 20-fold improvement in activity compared to the analogous amide, **6e**. However the most potent compounds in the key proliferation assay were found to be carboxamides containing a basic side chain exemplified by **6g** which demonstrated good activity in the HT-29 proliferation assay with an IC_{50} of 113 nM.

Encouraged by the promising initial SAR studies we sought to improve the synthetic route. In particular we wished to improve the overall yield and to identify routes which avoided the low yielding and capricious nucleophilic substitution reaction to introduce the aniline substituent.

Our improved synthetic route is described in Scheme 2. Key to the synthesis is the reaction between the easily obtained bromodione **7** and thiocarbamoyl intermediate **10**. Pleasingly the union between intermediates **7** and **10** proceeds smoothly in the presence of caesium carbonate to furnish directly ester **11** in moderate yield. Hydrolysis of the ester to the acid and subsequent amide formation occur in an identical manner to the previous synthesis. Alternatively the acid could be reacted with tetrafluorophenol resin and amides synthesized from the resultant resin-bound activated ester (step **g**). Importantly the new synthetic route allowed access to the 2-fluoro substituted anilines which were unobtainable by the previous methodology.

Activity data is presented in Table 2. The primary amide **13a** was sixfold more potent than the corresponding chloro analogue **6a** in the HT-29 proliferation assay, however aqueous solubility was still poor. The 3-hydroxypropyl carboxamide **13b** was synthesized to bind to the ATP region and demonstrated that moderate affinity was achieved in the cascade assay. However there was a 20-fold drop in potency when examined in the HT-29 proliferation assay (IC_{50} 6210 nM). This could have been due to the poor physico-chemical properties of the compound which resulted in a lack of cellular permeability. The corresponding ethylhydroxamate **13c** was prepared which improved the permeability of the compound in the proliferation assay 18-fold compared to the corresponding amide. It was expected that the hydroxypropyl hydroxamate **13d**

Table 1
Exploratory SAR for compounds **1**,**4** and **6a**–**g**[10]

Compound	R^1	Cascade IC_{50}	HT-29 pERK IC_{50}	HT-29 proliferation IC_{50}
1	n/a	946	1539	8869
4	O CH_2 CH_3	2617	NT	NT
6a	NH_2	13	92	596
6b	NH CH_3	226	224	1633
6c	Piperazine	456	45	1043
6d	*R*(-)-$NHCH_2CHOH(CH_2OH)$	28	43	710
6e	*R*(−)-$NH(CH_2)_2CHOH(CH_2OH)$	200	717	12110
6f	*R*(−)-$NHOCH_2CHOH(CH_2OH)$	9	76	896
6g	$NHCH_2C(CH_3)_2NH_2$	18	13	113

Values are means of two experiments. IC_{50} is quoted in nM. NT, not tested.

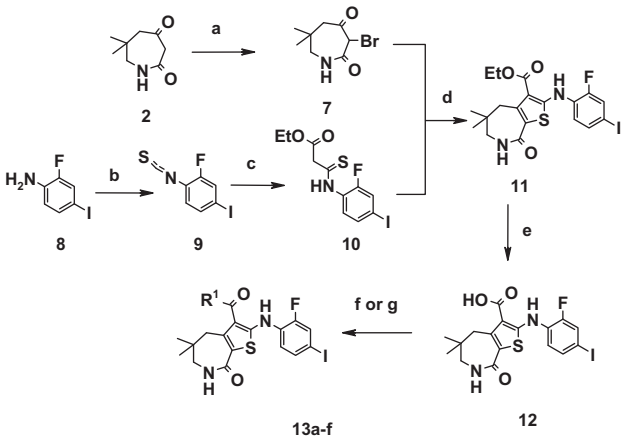

Scheme 2. Reagents and conditions: (a)NBS, $NaHSO_4$, THF, 25 °C, 81%; (b) Thiophosgene, $CHCl_3$, H_2O, 2-fluoro-4-iodoaniline, rt, 88%; (c) Ethylacetoacetate, NaOEt, EtOH, rt, 87%; (d) Cs_2CO_3, DMF, 80 °C, 43%; (e) LiOH, THF, H_2O, reflux, 79%; (f) amine R^1, EDC, NMM, HOBt, DMF, rt, 40–60%, (g) (i) tetrafluorophenol resin, DMF, DIC, DMAP, rt, (ii) amine R^1, THF, DMF, rt.

Table 2
Exploratory SAR for compounds **11**,**13a–h**[10]

Compounds	R^1	Cascade IC_{50}	HT-29 pERK IC_{50}, nM	HT-29 proliferation IC_{50}, nM
11	O CH_2 CH_3	305	NT	NT
12	OH	14	978	NT
13a	NH_2	9	NT	158
13b	$NH(CH_2)_2$ CH_2OH	309	140	6210
13c	$NHOCH_2CH_2OH$	7	18	340
13d	*R*-(−)-$NHOCH_2CHOH(CH_2OH)$	6	51	1578
13e	(*R*)-Piperidin-3-ylamine	22	5	91
13f	(*R*)-1-Pyrrolidin-2-yl-methylamine	42	22	120
13g	(*R*)-Pyrrolidin-3-ylamine	8	9	54
13h	$NHCH_2C(CH_3)_2NH_2$	14	6	79

Values are means of two experiments. IC_{50} is quoted in nM. NT, not tested.

would further improve the potency relative to the simple carboxamide. The hydroxamate **13d** was potent in the cascade assay, with an IC_{50} of 6 nM, however, the activity greatly diminished in the HT-29 proliferation assay (IC_{50} 1578 nM). The polar surface area of **13d** was 148 Å, resulting in poor cellular penetration. Incorporation of basic amides such as piperidine-3-ylamine **13e** or 2-methyl-propane-1,2-diamine **13h** led to good activity in the cascade assay which was maintained through into improved potencies in the HT-29 proliferation assay, **13h** (IC_{50} 79 nM).

A crystal structure of compound **13e** bound to MEK was obtained in the presence of AMPPNP-Mg^{2+} (Fig. 3).[17] The compound binds to MEK through a similar mode to the non-ATP competitive inhibitor **PD318088**. The structure reveals an electrostatic interaction between the 4′-iodide and backbone carbonyl of Val127 which is critical to the activity of the MEK inhibitors. Phe209 also forms an edge to face interaction with the 2-fluoro-4-iodoanilino ring. The carbonyl of the azepinone hydrogen bonds to the backbone NH of Val211, and the piperidin-3-ylamine terminal nitrogen interacts with the terminal phosphate of AMP-PNP. Gratifyingly the crystal structure confirmed our design hypothesis with the aryl iodide forming the key electrostatic interaction, the carbonyl group hydrogen bonding to the backbone and the 3-thiophenyl group interacting with AMP.

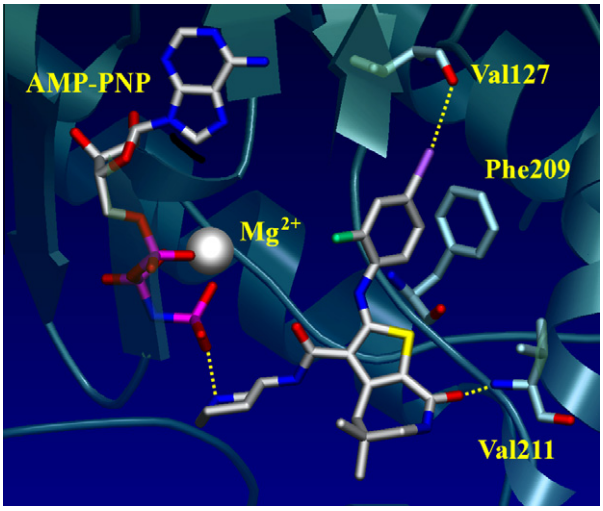

Figure 3. Crystal structure of compound **13e** bound to MEK-F11 with AMPPNP-Mg^2 (PDB code: 3SLS).

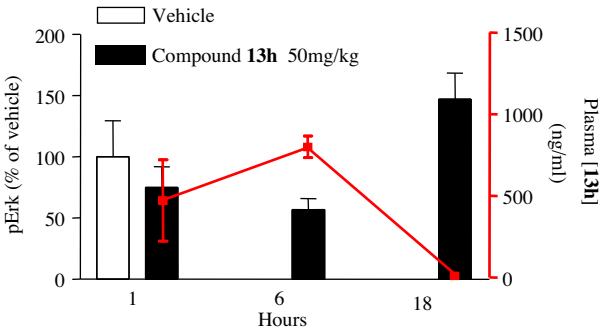

Figure 4. Time dependent reduction of pERK in HT-29 tumour bearing nude mice after treatment with compound **13h**. HT-29 tumour bearing mice were treated with vehicle (0 h) or 50 mg/kg compound p.o. pERK levels were measured 1, 6, 18 h post treatment. Drug plasma concentration was measured by LC–MS/MS.

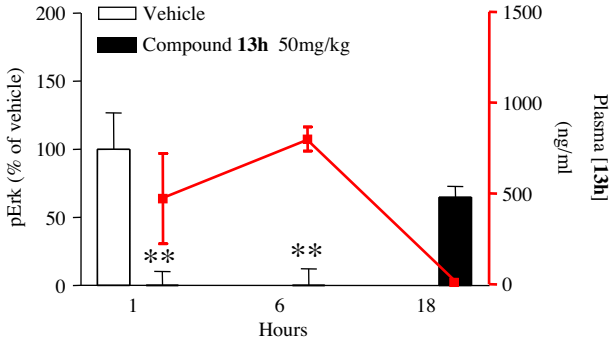

Figure 5. Time dependent reduction of pERK levels in PMA-stimulated whole blood in HT-29 tumour bearing nude mice after treatment with compound **13h**. HT-29 tumour bearing mice were treated with vehicle (0 h) or 50 mg/kg compound p.o. pERK levels were measured in whole blood 1, 6, 18 h post treatment. Drug plasma concentration was measured by LC–MS/MS. $^{**}p<0.01\%$ versus vehicle control, one-way ANOVA followed by Bonferroni post test.

Compound **13h** was selected for in vivo pharmacokinetic profiling based on its superior potency, good aqueous solubility (210 μM at pH 7.4) and low in vitro intrinsic clearance 2.6 μL/min/10^6 cells in rat hepatocytes. The in vivo pharmacokinetics of compound **13h** were assessed in female nude mice following a single p.o.

administration at 10 mg/kg. Compound **13h** had a C_{max} of 323 ng/mL and an AUC_{last} of 1239 ng h/mL and based on these data was progressed to PK/PD studies in nude mice bearing HT-29 tumours.

As seen in Figure 4, treatment with compound **13h**, 50 mg/kg p.o., resulted in inhibition of pERK in the HT-29 tumour. Within 1 h of dosing, pERK was reduced by 25% compared to control and this reduction increased at 6 h to 40% with pERK levels returning to control levels at 18 h. Analysis of plasma concentration show there was more compound present at the 6 h time point than at 1 h, and the compound was cleared by 18 h consistent with a slow absorption profile. Analysis of pERK inhibition in PMA-stimulated whole blood (Fig. 5), showed the complete knock down of pErk at 1 h which was maintained at 6 h, returning to a 35% reduction of pErk by 18 h. The greater inhibition of pERK in whole blood compared to tumour may be due to poor tumour penetration or the action of an efflux mechanism and has yet to be fully elucidated.

In conclusion a novel series of MEK inhibitors have been developed, and significant enzyme and cellular potency has been achieved across the series. Compounds with acceptable in vivo pharmacokinetic properties were identified and examined in a primary pharmacology model, demonstrating inhibition of pERK in both tumour and whole blood. Further optimisation and profiling of these compounds is ongoing.

Acknowledgments

We thank Caroline Hyden, Reena Halai and Tovah Shaw who performed the pErk and HT-29 proliferation assays and the DMPK team for bioanalysis support and in vivo PK.

References and notes

1. Ahn, N. G.; Seger, R.; Bratlien, R. L.; Diltz, C. D.; Tonks, N. K.; Krebs, E. G. *J. Biol. Chem.* **1991**, *266*, 4220.
2. Schaeffer, H. J.; Weber, M. *J. Mol. Cell. Biol.* **1999**, *19*, 2435.
3. Sebolt-Leopold, J. S. *Curr. Pharm. Des.* **2004**, *10*, 1907.
4. Montagut, C.; Settleman, J. *Cancer. Lett.* **2009**, *283*, 125.
5. Wang, J. Y.; Wilcoxen, K. M.; Nomoto, K.; Wu, S. *Curr. Top. Med. Chem.* **2007**, *7*, 1364.
6. Sebolt-Leopold, J. S.; Herrera, R. *Nat. Rev. Cancer.* **2004**, *4*, 937.
7. Ohren, J. F.; Chen, H.; Pavlovsky, A.; Whitehead, C.; Zhang, E.; Kuffa, P.; Yan, C.; McConnel, P.; Spressard, C.; Banotai, C.; Mueller, W. T.; Delaney, A.; Omer, C.; Sebolt-Leopold, J.; Dudley, D.; Leung, I.; Flamme, C.; Warmus, J. S.; Kaufman, M.; Barrett, S.; Tecle, H.; Hasemann; C *Nat. Struct. Mol. Biol* **2004**, *11*, 1192.
8. Alexander, R.; Balasundaram, A.; Batchelor, M.; Brookings, D.; Crépy, K.; Crabbe, T.; Deltent, M.; Dreissens, F.; Gill, A.; Harris, S.; Hutchinson, G.; Kulisa, C.; Merriman, M.; Mistry, P.; Parton, T.; Turner, J.; Whitcombe, I.; Wright, S. *Bioorg. Med. Chem. Lett.* **2008**, *18*, 4316.
9. Perry, B.; Alexander, R.; Bennett, G.; Buckley, G.; Ceska, T.; Crabbe, T.; Dale, V.; Gowers, L.; Horsely, H.; Lynwen, J.; Jenkins, K.; Crépy, K.; Kulisa, C.; Lightfoot, H.; Lock, C.; Mack, S.; Morgan, T.; Nicolas, A.; Pitt, W.; Sabin, V.; Wright, S. *Bioorg. Med. Chem. Lett.* **2008**, *18*, 4700.
10. Laing, V. E.; Brookings, D. C.; Carbery. R. J.; Gascon Simorte, J. M.; Hutchings, M. C.; Langham, B. J.; Lowe, M. A. WO 2008020206.
11. Razgulin, A. V.; Mecozzi, S. *J. Med. Chem.* **2006**, *49*, 7902.
12. Spicer, J. A.; Rewcastle, G. W.; Kaufman, M. D.; Black, S. L.; Plummer, M. S.; Denny, W. A.; Quin, J.; Shahripour, A. B.; Barrett, S. D.; Whitehead, C. E.; Milbank, J. B. J.; Ohren, J. F.; Gowan, R. C.; Omer, C.; Camp, H. S.; Esmaeil, N.; Moore, K.; Sebolt-Leopold, J.; Pryzbranowski, S.; Merriman, R. L.; Ortwine, D. F.; Warmus, J. S.; Flamme, C. M.; Tecle, H. *J. Med. Chem.* **2007**, *50*, 5090.
13. Gewald, K.; Schinke, E.; Böttcher, H. *Ber.* **1966**, *99*, 94.
14. Sabnis, R. W. *Sulfur Rep.* **1994**, *16*, 1.
15. Sabnis, R. W.; Rangnekar, D. W.; Sonawane, N. D. *J. Heterocycl. Chem.* **1999**, *36*, 333.
16. Barrett, S. D. et al *Bioorg. Med. Chem. Lett.* **2008**, *18*, 6501.
17. RCSB Protein Data Bank (PDB) database reference no. 3SLS.